

See discussions, stats, and author profiles for this publication at: <https://www.researchgate.net/publication/373019933>

VOLUME TWENTY FIVE ADVANCES IN BIOMEMBRANES AND LIPID SELF-ASSEMBLY

Chapter · August 2023

CITATIONS

0

2 authors:



Swathi Sudhakar

25 PUBLICATIONS 258 CITATIONS

SEE PROFILE



Poorni Balaji

Bulgarian Academy of Sciences

22 PUBLICATIONS 515 CITATIONS

SEE PROFILE

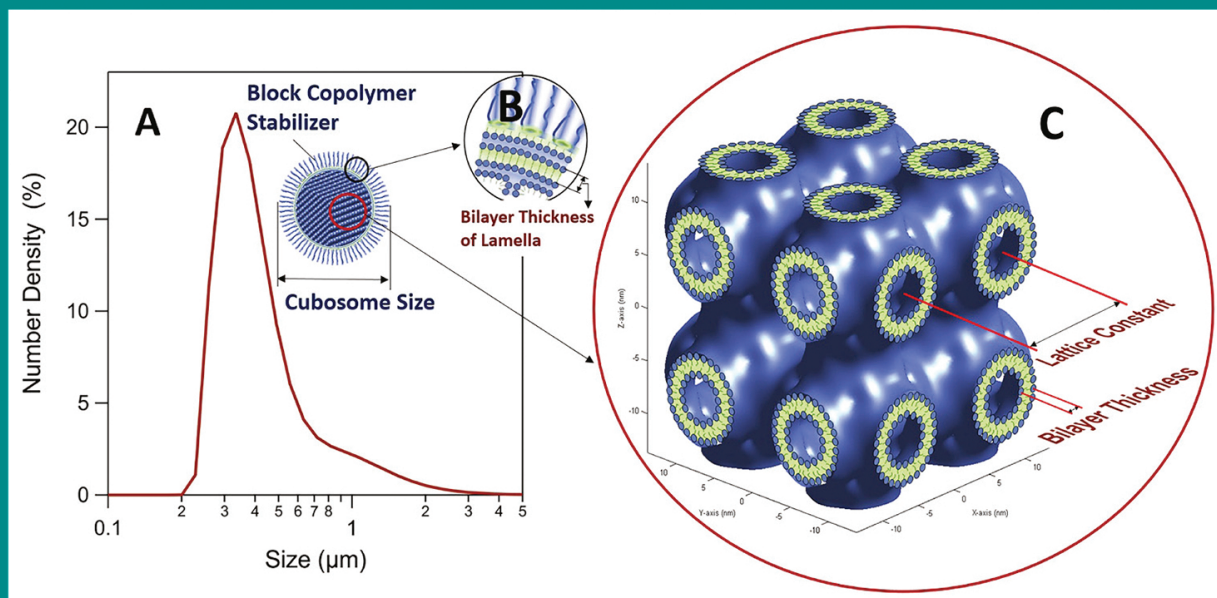
Some of the authors of this publication are also working on these related projects:



BioNanoscience [View project](#)

Advances in
**Biomembranes and
Lipid Self-Assemblies**

Volume 25



Edited by
**Aleš Iglič, Michael Rappolt
and Ana Garcia-Sáez**





VOLUME TWENTY FIVE

ADVANCES IN
**BIOMEMBRANES AND
LIPID SELF-ASSEMBLY**

EDITORIAL BOARD

- Dr. Mibel Aguilar** (*Monash University, Australia*)
Dr. Angelina Angelova (*Université de Paris-Sud, France*)
Dr. Paul A. Beales (*University of Leeds, United Kingdom*)
Dr. Habil. Rumiana Dimova (*Max Planck Institute of Colloids and Interfaces, Germany*)
Dr. Yuru Deng (*Changzhou University, China*)
Prof. Dr. Nir Gov (*The Weizmann Institute of Science, Israel*)
Prof. Dr. Wojciech Gózdź (*Institute of Physical Chemistry Polish Academy of Sciences, Poland*)
Prof. Dr. Thomas Heimburg (*Niels Bohr Institute, University of Copenhagen, Denmark*)
Prof. Dr. Tibor Hianik (*Comenius University, Slovakia*)
Dr. Chandrashekhhar V. Kulkarni (*Centre for Materials Science, University of Central Lancashire, Preston, United Kingdom*)
Prof. Dr. Angelica Leitmannova Liu (*USA*)
Dr. Ilya Levental (*University of Texas, USA*)
Prof. Dr. Reinhard Lipowsky (*MPI of Colloids and Interfaces, Potsdam, Germany*)
Prof. Dr. Sylvio May (*North Dakota State University, USA*)
Prof. Dr. Philippe Meleard (*Ecole Nationale Supérieure de Chimie de Rennes, France*)
Prof. Dr. Yoshinori Muto (*Gifu, Japan*)
V. A. Raghunathan (*Raman Research Institute, India*)
Dr. Amin Sadeghpour (*University of Leeds, United Kingdom*)
Prof. Kazutami Sakamoto (*Chiba Institute of Science, Japan*)
Prof. Dr. Bernhard Schuster (*University of Natural Resources and Life Sciences, Vienna*)
Prof. Dr. P.B. Sunil Kumar (*Indian Institute of Technology Madras, India*)
Prof. Dr. Mathias Winterhalter (*Jacobs University Bremen, Germany*)

VOLUME TWENTY FIVE

ADVANCES IN BIOMEMBRANES AND LIPID SELF-ASSEMBLY

Edited by

PROFESSOR DR. ALEŠ IGLIČ

*Laboratory of Biophysics, Faculty of Electrical Engineering,
University of Ljubljana, Ljubljana, Slovenia*

PROFESSOR DR. ANA GARCIA-SÁEZ

*Universität Tübingen
Interfakultäres Institut für Biochemie (IFIB)
Hoppe-Seyler-Str. 4
72076 Tübingen, Germany*

PROFESSOR DR. MICHAEL RAPPOLT

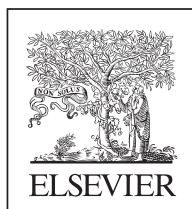
*School of Food Science and Nutrition,
University of Leeds, United Kingdom*

Founding Editors

PROFESSOR DR. H.T. TIEN

PROFESSOR DR. A. OTTOVA-LEITMANNOVA

Michigan State University, USA



ACADEMIC PRESS

An imprint of Elsevier

Academic Press is an imprint of Elsevier
50 Hampshire Street, 5th Floor, Cambridge, MA 02139, United States
525 B Street, Suite 1800, San Diego, CA 92101-4495, United States
The Boulevard, Langford Lane, Kidlington, Oxford OX5 1GB, United Kingdom
125 London Wall, London, EC2Y 5AS, United Kingdom

First edition 2017

Copyright © 2017 Elsevier Inc. All rights reserved.

No part of this publication may be reproduced or transmitted in any form or by any means, electronic or mechanical, including photocopying, recording, or any information storage and retrieval system, without permission in writing from the publisher. Details on how to seek permission, further information about the Publisher's permissions policies and our arrangements with organizations such as the Copyright Clearance Center and the Copyright Licensing Agency, can be found at our website: www.elsevier.com/permissions.

This book and the individual contributions contained in it are protected under copyright by the Publisher (other than as may be noted herein).

Notices

Knowledge and best practice in this field are constantly changing. As new research and experience broaden our understanding, changes in research methods, professional practices, or medical treatment may become necessary.

Practitioners and researchers must always rely on their own experience and knowledge in evaluating and using any information, methods, compounds, or experiments described herein. In using such information or methods they should be mindful of their own safety and the safety of others, including parties for whom they have a professional responsibility.

To the fullest extent of the law, neither the Publisher nor the authors, contributors, or editors, assume any liability for any injury and/or damage to persons or property as a matter of products liability, negligence or otherwise, or from any use or operation of any methods, products, instructions, or ideas contained in the material herein.

ISBN: 978-0-12-812080-4

ISSN: 2451-9634

For information on all Academic Press publications
visit our website at <https://www.elsevier.com/books-and-journals>



Publisher: Zoe Kruze

Acquisition Editor: Poppy Garraway

Editorial Project Manager: Shellie Bryant

Production Project Manager: Magesh Kumar Mahalingam

Cover Designer: Greg Harris

Typeset by SPi Global, India

CONTENTS

<i>Contributors</i>	<i>ix</i>
<i>Preface</i>	<i>xi</i>
1. Could Titanium Dioxide Nanotubes Represent a Viable Support System for Appropriate Cells in Vascular Implants?	1
I. Junkar, M. Kulkarni, P. Humpolíček, Z. Capáková, B. Burja, A. Mazare, P. Schmuki, K. Mrak-Poljšak, A. Flašker, P. Žigon, S. Čučnik, M. Mozetič, M. Tomšič, A. Iglič, and S. Sodin-Semrl	
1. Introduction	2
2. Selected Clinical Conditions Associated With Vessel Implants	3
3. Types of Vascular Implants	6
4. Nanotopography, Surface Modifications, and Biocompatibility of Implants	11
5. TiO ₂ Nanotubes	14
6. Surface Modification of TiO ₂ Nanotubes	19
7. Interaction of TiO ₂ Nanotubes With Cells	22
8. Antiinfective Properties of TiO ₂ Nanotubes	32
9. Concluding Remarks and Perspectives	33
References	34
2. Ras Proteolipid Nanoassemblies on the Plasma Membrane Sort Lipids With High Selectivity	41
Y. Zhou and J.F. Hancock	
1. Ras Proteins Are Lipid-Anchored and Form Nanoclusters on Cell Plasma Membrane	42
2. Ras Nanoclusters Act as Nanoswitches to Transiently Regulate MAPK Signal Transduction	45
3. Ras Nanoclusters Preferences for Ordered vs Disordered Domains in Cell PM	47
4. Acidic Lipid Selectivity of Ras Nanoclusters	50
5. Perturbation of Ras Nanoclusters Alters Ras Effector Binding and Signaling	56
6. Conclusion	58
Acknowledgment	58
References	58

3. Membrane-Mimetic Inverse Bicontinuous Cubic Phase Systems for Encapsulation of Peptides and Proteins	63
T.G. Meikle, C.J. Drummond, F. Separovic, and C.E. Conn	
1. Inverse Bicontinuous Cubic Phases	64
2. Peptide and Protein Encapsulation: Understanding the Structural Relationship Between Guest Molecules and the Cubic Phase	66
3. Lipid Packing, Interfacial Curvature, and Lateral Pressure	67
4. Applications of Bicontinuous Cubic Phases for Protein or Peptide Encapsulation	69
5. Cubic Phase Nanoparticles (Cubosomes)	71
6. Characterization of Bicontinuous Cubic Phase-Peptide/Protein Systems	73
7. Conclusion	87
Acknowledgments	88
References	88
4. Interactions of Flavonoids With Lipidic Mesophases	95
A. Sadeghpour, D. Sanver, and M. Rappolt	
1. Introduction	96
2. Flavonoids Interacting With Planar Membranes	97
3. Flavonoids Interacting With Curved Membranes	108
4. Conclusions	116
Acknowledgment	117
References	117
5. Preparation and Characterization of Supported Lipid Bilayers for Biomolecular Interaction Studies by Dual Polarization Interferometry	125
T.-H. Lee and M.-I. Aguilar	
1. Introduction	126
2. Dual Polarization Interferometry	129
3. Experimental Protocols for Solid-Supported Membranes in DPI Analysis	136
4. Changes in Lipid Molecular Organization in Relation to the Solute–Membrane Interaction	147
5. Summary and Outlook	152
References	152
6. Gold Nanomaterials: Recent Advances in Cancer Theranostics	161
S. Sudhakar and P.B. Santhosh	
1. Introduction to Different Forms of Gold Nanomaterials	162
2. Synthesis of Different Forms of Gold Nanomaterials	164

3. Diagnostic and Imaging Applications of Gold Nanomaterials	170
4. Therapeutic and Drug Delivery Applications of Gold Nanomaterials	171
5. Conclusion and Perspectives	173
References	173
<i>Index</i>	181

This page intentionally left blank

CONTRIBUTORS

M.-I. Aguilar

Monash University, Clayton, VIC, Australia

B. Burja

University Medical Centre Ljubljana, Ljubljana, Slovenia

Z. Capáková

Centre of Polymer Systems, Tomas Bata University in Zlin, Zlin, Czech Republic

S. Čučnik

University Medical Centre Ljubljana; Faculty of Pharmacy, University of Ljubljana, Ljubljana, Slovenia

C.E. Conn

School of Science, College of Science, Engineering and Health, RMIT University, Melbourne, VIC, Australia

C.J. Drummond

School of Science, College of Science, Engineering and Health, RMIT University, Melbourne, VIC, Australia

A. Flašker

Chemical Institute, Ljubljana, Slovenia

J.F. Hancock

McGovern Medical School, University of Texas Health Science Center, Houston, TX, United States

P. Humpolíček

Centre of Polymer Systems, Tomas Bata University in Zlin, Zlin, Czech Republic

A. Iglič

Laboratory of Biophysics, Faculty of Electrical Engineering, University of Ljubljana, Ljubljana, Slovenia

I. Junkar

Josef Stefan Institute, Ljubljana, Slovenia

M. Kulkarni

Laboratory of Biophysics, Faculty of Electrical Engineering, University of Ljubljana, Ljubljana, Slovenia

T.-H. Lee

Monash University, Clayton, VIC, Australia

A. Mazare

Chair of Surface Science and Corrosion, University of Erlangen–Nuremberg, Erlangen, Germany

T.G. Meikle

School of Chemistry, Bio21 Institute, University of Melbourne, Melbourne, VIC, Australia

M. Mozetič

Josef Stefan Institute, Ljubljana, Slovenia

K. Mrak-Poljšak

University Medical Centre Ljubljana, Ljubljana, Slovenia

M. Rappolt

School of Food Science and Nutrition, University of Leeds, Leeds, United Kingdom

A. Sadeghpour

School of Food Science and Nutrition, University of Leeds, Leeds, United Kingdom

P.B. Santhosh

Indian Institute of Technology, Chennai, India

D. Sanver

School of Food Science and Nutrition, University of Leeds, Leeds, United Kingdom

P. Schmuki

Chair of Surface Science and Corrosion, University of Erlangen–Nuremberg, Erlangen, Germany

F. Separovic

School of Chemistry, Bio21 Institute, University of Melbourne, Melbourne, VIC, Australia

S. Sodín-Semrl

University Medical Centre Ljubljana, Ljubljana; Faculty of Mathematics, Natural Science and Information Technologies, University of Primorska, Koper, Slovenia

S. Sudhakar

Centre for Biotechnology, Anna University, Chennai, India

M. Tomšič

University Medical Centre Ljubljana; Faculty of Medicine, University of Ljubljana, Ljubljana, Slovenia

Y. Zhou

McGovern Medical School, University of Texas Health Science Center, Houston, TX, United States

P. Žigon

University Medical Centre Ljubljana, Ljubljana, Slovenia



Gold Nanomaterials: Recent Advances in Cancer Theranostics

S. Sudhakar*, P.B. Santhosh^{†,1}

*Centre for Biotechnology, Anna University, Chennai, India

[†]Indian Institute of Technology, Chennai, India

¹Corresponding author: e-mail address: poorni_balaji@yahoo.com

Contents

1. Introduction to Different Forms of Gold Nanomaterials	162
1.1 Gold Nanoparticles	162
1.2 Gold Nanorods	163
1.3 Gold Nanocages	163
1.4 Gold Nanoshells	164
1.5 Gold Nanostars	164
2. Synthesis of Different Forms of Gold Nanomaterials	164
2.1 Chemical-Mediated Synthesis of Gold Nanomaterials	164
2.2 Green Synthesis of Gold Nanomaterials	167
2.3 Microbial Synthesis of Gold Nanomaterials	168
3. Diagnostic and Imaging Applications of Gold Nanomaterials	170
4. Therapeutic and Drug Delivery Applications of Gold Nanomaterials	171
5. Conclusion and Perspectives	173
References	173

Abstract

This chapter describes the potential of various shapes of gold nanomaterials such as nanoparticles, nanorods, nanostars, nanocages, and nanoshells in cancer nanotheranostics, i.e., both as diagnostic and therapeutic agent. This study includes the synthesis of different gold nanomaterials using several methods like chemical, green-, and microbial-mediated synthesis. The ability of gold nanomaterials to absorb light in the near-infrared region and transform it into heat and their unique optical properties make them a promising tool in photothermal cancer therapy. Herein, we present the recent advances and the ability of gold nanomaterials to show its multiple roles in the field of cancer biology.



1. INTRODUCTION TO DIFFERENT FORMS OF GOLD NANOMATERIALS

Gold nanomaterials have gained huge interest in various biomedical applications and considered to have a promising potential in the field of cancer biology. Based on the synthesis procedure and experimental conditions, various shapes of gold nanomaterials including spherical gold nanoparticles, nanorods, nanoshells, nanocages, nanostars, nanoboxes, nanocubes, nanocrystals, and triangular bipyramids have been investigated [1–7]. In this chapter about gold nanomaterials, first we are going to have a look on synthesis of different shapes of gold nanomaterials and applications as diagnostic and therapeutic agents in cancer.

1.1 Gold Nanoparticles

When compared to many other metallic nanoparticles, noble metals like gold nanoparticles (AuNPs) have distinct electronic and optical properties. When the AuNPs are excited by light at specific wavelengths, the incident photons interact strongly with the conduction band of electrons and cause them to oscillate with resonant frequency. This collective oscillation is known as localized surface plasmon resonance (LSPR) which creates strong and localized electromagnetic fields and allows sensitive detection of changes in dielectric environment surrounding the nanoparticle surface. This property makes them to be prominently utilized in imaging, drug delivery, cosmetics, and in cancer theranostic applications [8,9]. The AuNPs display various colors based on their shape, size, and amount of aggregation of particles [10]. The AuNPs are evolving as an innovative platform for both, cancer targeted imaging and drug delivery usually represented as theranostic application. When irradiated with near-infrared (NIR) light, they induce hyperthermia (increased temperature to kill cancer cells) [11,12]. Furthermore, AuNPs could be successfully and selectively delivered to malignant and benign tumors and could act as carriers for chemotherapeutic drugs like curcumin, and paclitaxel in cancer treatment [13]. Apart from therapeutic applications, AuNPs are employed as imaging agents and biosensors due to their capability to emit photons upon irradiation. The gold nanomaterials of different shapes are schematically represented in Fig. 1.

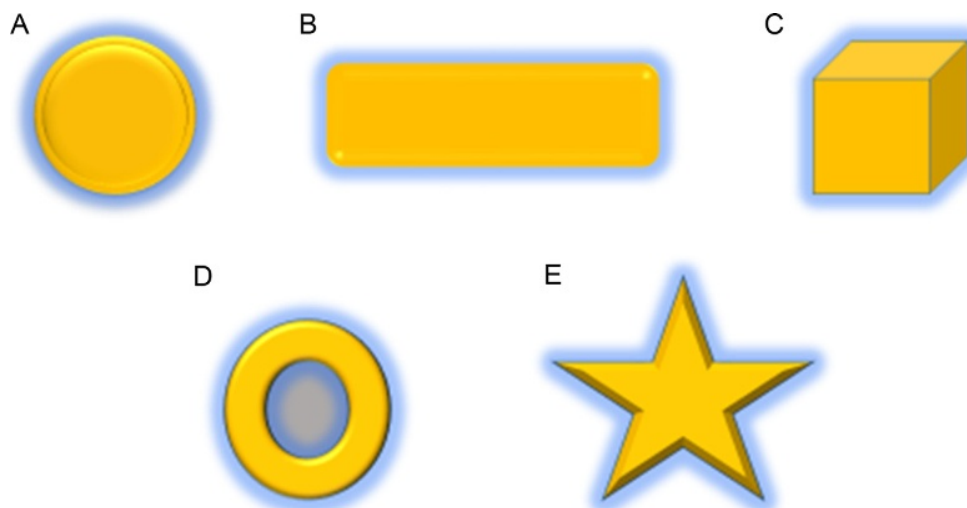


Fig. 1 Schematic presentation of differently shaped gold nanoparticles: (A) nanosphere, (B) nanorod, (C) nanocube, (D) nanoshell, and (E) nanostar.

1.2 Gold Nanorods

When compared to spherical gold particles, the AuNRs have drawn worldwide attention because of their inimitable shape-dependent optical properties. What makes the AuNRs as exclusive materials for biological imaging, sensing, photo thermal therapy, and drug delivery is their ability to possess different plasmon bands [14–17]. Even though, they have attracting features, their usage is restricted because even a small change in the shape, size, and surface nature will alter their properties which in turn affect their biological applications. The major advantages of using AuNRs include their surface plasmon resonance extinction in the NIR region which makes their use appropriately in the medical field for photo thermal therapy, biological sensing, and imaging.

1.3 Gold Nanocages

Next, we move on to a novel nanostructure called gold nanocages (AuNCgs) which are usually characterized by the ultrathin porous walls and hollow interiors. Usually they are prepared by keeping the silver nanoparticles as templates which involves galvanic replacement reaction [18–20]. The penetration depth of light can be maximized in soft tissues, by limiting the light source to NIR region from 650 to 900 nm, where the absorption by hemoglobin and water is negligible. To make AuNCgs suitable for this application, the LSPR peaks can be concisely tuned throughout the visible and NIR regions [21–24]. Prevalently, AuNCgs

are also functionalized with biological molecules to target cancer cells for both photothermal therapy and diagnosis at an early stage [25,26].

1.4 Gold Nanoshells

Gold nanoshells (AuNShs) are composed of a silica core coated by a thin gold metallic shell. One of the interesting properties about the AuNShs is their unique surface plasmon resonance property which can be finely tuned ranging from visible to NIR region. Multiple templates are employed for the formation of hollow AuNShs which includes silica particles [27], metal particles [28–31], etc. The AuNShs have demonstrated their potential in a variety of biomedical applications ranging from substrates for whole-blood immunoassays to photothermal cancer therapy [32–34]. By using magnetic resonance thermal guidance, *in vitro* cancer cells were successfully ablated using AuNShs. Similar use of AuNShs for photothermal ablation of tumors in mice showed complete regression of tumors with the mice remaining healthy compared with the controls [35–38].

1.5 Gold Nanostars

The gold nanostars (AuNSts) have multiple sharp branch structure which sharply increases the electromagnetic field. The AuNSts also have unique plasmon bands which are tunable from visible to NIR region. The fabrication of AuNSts has been driven by the interest on the LSPR response to the environment, especially on sharp tips and edges, where light can be highly concentrated [39–43]. Because of their exclusive property, they serve as effective tools in the field of nanomedicine. Furthermore, AuNSts also display stronger surface-enhanced resonance spectrum activity than gold spheres or even rods.



2. SYNTHESIS OF DIFFERENT FORMS OF GOLD NANOMATERIALS

2.1 Chemical-Mediated Synthesis of Gold Nanomaterials

2.1.1 Synthesis of Gold Nanoparticles

The simplest protocol commonly used for the groundwork of AuNPs is the facile reduction of gold salt in aqueous medium using sodium citrate [44,45], in which Au^{3+} ions are reduced to neutral gold atoms which slowly precipitates to form nanometer-sized gold particles. The widely used reducing agents for the synthesis of AuNPs include aminoboranes, borohydrides, hydrazine, hydroxylamine, formaldehyde, polyols, sugars, saturated and

unsaturated alcohols, hydrogen peroxide, citric and oxalic acids, carbon monoxide, sulfites, acetylene, and hydrogen [46–48]. A variety of stabilizers such as phosphorus ligands, trisodium citrate dihydrate, nitrogen-based ligands, sulfur ligands, dendrimers, oxygen-based ligands, polymers, and surfactants are used to impart the colloidal stability to AuNPs [49,50]. Synthesis of AuNPs by citrate-stabilized method, introduced by Turkevich, is the most popular method in which trisodium citrate dihydrate is added to the boiling chloroauric acid under vigorous stirring, leading to the formation of wine-red colloidal suspension after a few minutes [51,52]. To improve this method, Frens altered the ratio of gold and trisodium citrate, resulting in the synthesis of AuNPs of wide size range (from 15 to 150 nm) [46]. The size of the AuNPs obtained using Brust–Schiffrin method ranges from 2 to 5 nm, which is much smaller in size than particles synthesized by Turkevich method. Another popular technique for synthesis of AuNPs is seed growth method where one can easily control the size and shape of the particle. Usually, it involves two steps, preparation of small sized AuNPs followed by addition of seeds to the growth solution.

2.1.2 Synthesis of Gold Nanorods

In general, AuNRs are produced using cetyltrimethyl ammonium bromide (CTAB) which acts as both reducing and stabilizing agent to produce homogeneous AuNRs with high yield [53–56,4,57–61]. The LSPR resonances of AuNRs are generally observed both in the visible and NIR region [62–70]. Since CTAB is cytotoxic, various biocompatible agents like proteins and lipids are being used to provide stability, reduce cytotoxicity, and to retain its properties. A number of studies have focused on surface modification of AuNRs to address the above mentioned issues. An intrinsic problem in the synthesis of AuNRs using conventional method is its meager efficiency to convert chloroauric acid into nanorods. Reports have shown that only 15% of gold seeds are usually converted into the rods. The AuNRs yield could be increased by preparing the AuNRs in consecutive supernatant solutions. There is an urgent need for novel synthetic protocols in order to make the synthesis process more scalable and efficient as AuNRs progress greatly toward commercial applications.

2.1.3 Synthesis of Gold Nanocages

Recently, AuNCgs with hollow interiors, porous walls, and tunable LSPR in the NIR region have become a new promising platform for therapeutic applications. The unique structures of AuNCgs make them well suited for

drug encapsulation and photothermal controlled drug release with high spatial and temporal resolution. The AuNCs are generally synthesized through a simple galvanic replacement reaction between solutions containing salts of metal precursors and Ag nanostructures prepared through polyol reduction. The reduced metal deposits on the surface of the AuNCs, adopting their underlying cubic form. Concurrent with this deposition, the interior Ag is oxidized and removed, together with alloying and dealloying, AuNCs are produced. [71].

2.1.4 Synthesis of Gold Nanoshells

The commonly used method for the synthesis of gold nanoshells (AuNShs) involves the reduction of chloroauric acid with ascorbic acid at ambient temperature on presynthesized gold nanoseeds and in the presence of surfactants (in most cases CTAB). A general one-pot synthetic strategy for the synthesis of hollow AuNShs includes the reduction of chloroauric acid in 3-aminopropyltriethoxysilane in water suspension [72]. The AuNShs show a high photothermal conversion efficiency (up to 45%) and excellent stability under laser irradiation.

2.1.5 Synthesis of Gold Nanostars

The AuNSTs are synthesized by anisotropic growth process, by altering the growth rates along the specific crystallographic directions [73]. The shape of AuNSTs could be controlled by varying the concentration of silver nitrate. The stirring speed, pH, and the ratios of ascorbic acid, silver nitrate, and chloroauric acid determine the size and shape of the AuNSTs. Murphy and coworkers have studied the influence of reducing agent by replacing bromide ions of CTAB with its chloride equivalent to achieve a better control over size [74]. Few groups have used hydroxylamine sulfate in the preparation of polycrystalline-branched AuNSTs in a stepwise growth approach with sizes ranging from 48 up to 186 nm [75]. It is also reported that addition of polyvinyl pyrrolidone with 15 nm chloroauric acid solution leads to the formation of highly branched AuNSTs [76]. Recently, a simple one-step synthesis of AuNSTs using hydroxylamine as a reducing agent was reported [77]. The controlled synthesis of high-yield AuNSTs ranging from 45 to 116 nm was reported by Khoury and Vo-Dinh [78]. The AuNSTs were synthesized by extending the protocol reported by Liz-Marzan *et al.* [79], in order to enable size control of the stars from approximately 45 to 116 nm in size. This size range translates to tuning capabilities of the longitudinal plasmon peak in the NIR region from around 725 to 850 nm. They have used 20 nm

polyvinylpyrrolidone-coated gold seeds in ethanol and investigated the growth of AuNSts as a function of time during the synthesis by monitoring the spectrum of the AuNSts suspension and by imaging morphological changes of stars from time to time via transmission electron microscopy.

2.2 Green Synthesis of Gold Nanomaterials

Even though there are several methods like thermal decomposition, sonochemical, microwave irradiation, chemical reduction, electrochemical ablation for the synthesis of gold nanomaterials, many of these routine methods use hazardous chemicals. Hence, synthesis of nanoparticles in an ecofriendly way is essential. The green synthesis method is more advantageous when compared to other conventional methods which requires extended and high cost for downstream processing. The main components in plants responsible for the reduction of gold ions are usually phenols, proteins, and flavonoids which also acts as a stabilizing agent by capping the nanoparticles. Researchers have explored industrially and botanically important plants for the synthesis of nanoparticles. The active ingredients present in the plant extracts will provide special surface characteristics to the nanoparticles. Citrus maxima fruit extracts are widely used for the inexpensive synthesis of AuNPs [80]. Ghodake *et al.* [81] demonstrated casein hydrolytic peptides (CHPs)-mediated synthesis of crystalline AuNPs. The mechanism behind the nanoparticle formation is attributed to the catalytic properties of hydroxyl groups present in the CHPs. The CHPs are capable of forming a monolayer on the surface of AuNPs via electrostatic interactions, thus playing an important role in long-term stability. Yana *et al.* [82] reported a facile, one-pot green synthesis of biomaterial-supported AuNPs using cellulose with superior catalytic activity. In general, cellulose-mediated AuNPs with a size range of 5–10 nm are prepared by heating the aqueous mixture of chloroauric acid, with cellulose and poly ethylene glycol. Nazirova *et al.* [83] reported water-soluble luminescent AuNPs with average size 2.3 nm synthesized from *N*-(4-imidazolyl) methylchitosan. The biological activity of imidazolyl-containing polymers and their capability to bind proteins and drugs have huge applications in the field of bioimaging, biomolecules detection, catalysis, and drug delivery. Suarasana *et al.* [84] reported the one-pot, green synthesis of AuNPs using gelatin biopolymer having unique reducing, stabilizing, and eminent growth controlling ability. Sadeghi *et al.* [85] reported that the plant *Stevia rebaudiana* have higher amount of polyphenols and flavonoids which makes them more

Table 1 Green Synthesis of Gold Nanoparticles Using Different Plant Sources

Plants	Size of the Particle (nm)	Shapes	References
<i>Acanthella elongata</i>	15	Spherical	[87]
<i>Sugar beet pulp</i>	20	Triangular	[88]
<i>Cinnamomun zylanicum</i>	20	Spherical	[89]
<i>Zingiber officinale</i>	5–15	Spherical	[90]
<i>Olive leaf extract</i>	50–100	Spherical, triangular	[91]
<i>Coriander leaf extract</i>	6–58	Spherical, triangular	[92]
<i>Cassia auriculata</i>	38	Spherical, triangular	[93]
<i>Hibiscus rosasinensis</i>	15–25	Spherical, triangular, hexagonal	[94]
<i>Terminalia chebula</i>	50–100	Spherical	[95]
<i>Rosa hybrida</i>	35	Spherical	[96]
<i>Morinda citrifolia</i>	10–40	Triangular	[97]
<i>Tamarind leaf extract</i>	20	Spherical	[98]
<i>Palm oil mill effluent</i>	50	Spherical	[99]

specific to act as reducing agent in the synthesis of AuNPs. Yuan *et al.* [86] reported a facile and rapid a single-pot synthesis process for AuNPs using capsicum. The synthesis of AuNps of various shapes from different plant sources is shown in Table 1.

2.3 Microbial Synthesis of Gold Nanomaterials

Synthesis of nanomaterials using microorganisms is an emerging field of industrial microbiology. Biological approaches using either unicellular or multicellular organisms for the synthesis of gold nanomaterials are simple, viable, and ecofriendly alternate to chemical methods. Different biological entities like bacteria, fungi, algae, yeast, and plants are drastically studied for their ability to synthesize metal nanoparticles for various pharmacological applications (Table 2) [109].

There are two ways by which AuNPs can be synthesized by microbes, either extracellularly or intracellularly. The most popular method is extracellular synthesis, as it eliminates numerous downstream processing steps

Table 2 Microbial Synthesis of Gold Nanoparticles of Different Sizes

Microorganism	Size of the Particle (nm)	References
<i>Bacillus subtilis</i>	5–25	[100]
<i>Sulfate-reducing bacteria</i>	15–200	[101]
<i>Shewanella algae</i>	10	[102]
<i>Escherichia coli</i> DH5 α	10–20	[103]
<i>Pseudomonas stutzeri</i>	200	[104]
<i>Corynebacterium</i>	10	[105]
<i>Rhodobacter</i>	10–20	[106]
<i>Bacillus</i> sp.	10	[107]
<i>Pseudomonas aeruginosa</i>	17.2	[108]

during the synthesis. The usual procedure followed is to centrifuge the second day well-grown culture to discard the biomass and add the supernatant to chloroauric acid. The enzymes like NADH dehydrogenase, NADPH-dependent sulfite reductase in the microbes act as reducing agents [110]. After bioreduction, the AuNPs can be collected by similar methodologies as in plant extract-mediated synthesis. Cell-free viable approach for synthesis of AuNPs using *Escherichia coli* has also been reported [111]. Despite the stability, biological nanoparticles are usually not monodisperse, and the rate of synthesis is slow. To overcome these problems, several factors such as microbial cultivation methods and the extraction techniques have to be optimized, and the combinatorial approach such as photobiological methods may be used. In the case of intracellular-mediated synthesis process, the particles are released to the external environment either by ultrasound treatment or by adding apt detergents. *Geobacter ferrireducens*, a Fe (III) reducing bacterium, reduces and precipitates the gold in periplasmic space intracellularly. Similarly, in the presence hydrogen gas microbes like *Shewanella algae*, mesophilic bacteria reduce Au^{+3} ions in anaerobic conditions. *Plectonema boryanum*, a filamentous cyanobacterium, precipitates AuNPs in abiotic and cyanobacterial systems. *Escherichia coli* DH5 α -mediated bioreduction of chloroauric acid to Au^0 nanoparticles has been reported recently [112]. The accumulated particles on the cell surface were mostly spherical. These cell-bound nanoparticles have been reported for promising applications in realizing the direct electrochemistry of hemoglobin and other proteins [113]. Similarly, the bioreduction of trivalent aurum was also reported in

photosynthetic bacterium, *Rhodobacter capsulatus* which showed biosorption capacity of 92.43 mg chloroauric acid/g dry weight in the logarithmic phase of its growth. The carotenoids and NADPH-dependent enzymes embedded in plasma membrane and/or secreted extracellularly were found to be involved in the biosorption and bioreduction of Au^{+3} to Au^0 on the plasma membrane and also extracellularly [100]. Owing to the rich biodiversity of microbes, their potential as biological materials for nanoparticle synthesis is yet to be fully explored.



3. DIAGNOSTIC AND IMAGING APPLICATIONS OF GOLD NANOMATERIALS

As discussed earlier, gold nanomaterials have unique properties which attract researchers to focus their studies in the field of tumor molecular imaging and diagnostics. Herein, Zhou and Jia [114] reported a facile approach in which polyethylenimine (PEI) modified with polyethylene glycol (PEG), a cost effective template, is used for the synthesis of folic acid (FA)-targeted multifunctional AuNPs. The PEI was consecutively modified with FA-linked PEG, PEG monomethyl ether and with fluorescein isothiocyanate for the synthesis of AuNPs. The prepared AuNPs were noncytotoxic and colloidally stable. They acted as novel nanoprobe for targeted CT imaging of FAR-expressing cancer cells. Lozano *et al.* [115] demonstrated the hybrid vesicular systems composed of liposomes and AuNRs aid in deep tissue detection, therapy, and monitoring in living animals using multispectral optoacoustic tomography [116].

Gallina *et al.* [117] reported that fluorescent, biocompatible, aptamer-conjugated AuNRs act as perfect agents for diagnostics and therapeutics. Bioconjugation of AuNRs with anticancer oligonucleotide AS1411 was employed and the aptamer-conjugated AuNRs acted as ideal cancer-selective multifunctional probes for imaging. Huang *et al.* [12] reported the synthesis of multifunctional nanoprobe in which silica functionalized gold was decorated with FA molecule which displayed strong computed tomography imaging and X-ray attenuation. Vo-Dinh and coworkers reported the synthesis of AuNSTs for *in vivo* imaging with adjustable geometry. They exhibited strong two-photon photoluminescence process which is confirmed by the quadratic dependence of the luminescence signal up to excitation power which may originate from electron-hole-recombination. They also reported TPL imaging on BT549 cancer cells by wheat germ agglutinin-functionalized AuNSTs for imaging.

The reconstituted images appeared white due to the emission of red, blue, and green channels by AuNSts [118].

Tracking of AuNPs needs some fluorescent label but the imaging and tracking of AuNSts are possible without the need of fluorophores due to their unique strong two-photon action cross sections (TPACS) [119]. Due to the high TPACS of nanostars, tracking the motion of PEGylated AuNSts in blood vessels is also possible. In medicine, novel techniques with high specificity, such as positron emission tomography, require probe labeling and offer low spatial resolution which can be obtained by AuNSts. Photoacoustic microscopy is an emerging imaging modality that combines both rich optical absorption and high ultrasonic resolution in a single-imaging modality [120], and it is based on the use of highly absorbance nanoparticles. It also provides *in vivo* functional imaging information at clinically relevant penetration depths. Recently, AuNSts have been effectively used as enhancing agents in photoacoustic imaging [121].

Nie and coworkers reported the three-dimensional image reconstruction using AuNSts [122]. The AuNSts conjugated with cyclic RGD (Arg-Gly-Asp) peptides and anticancer drug doxorubicin (DOX) were studied in different tumor cell lines, and *in vivo* imaging was done using S180 tumor-bearing mouse model cells (MDA-MB-231) [123]. The fluorescence images of Au-RGD-DOX after incubating with MDA-MB-231 cells for 8 h were collected in order to understand the intracellular kinetics of the multifunctional nanoparticles. The obtained data clearly indicated that Au-RGD-DOX or released DOX entered the nucleus with only a small fraction remaining in the cytoplasm. The AuNSts with size less than 100 nm can accumulate selectively in tumors via the enhanced permeability and retention effect which is due to the increased leakiness of blood vasculature in tumors [124–126]. Combining this statement and their unique properties, AuNSts are considered to be suitable platforms for multimodal imaging for cancer diagnostics.



4. THERAPEUTIC AND DRUG DELIVERY APPLICATIONS OF GOLD NANOMATERIALS

From spheres to rods, different geometrical configurations of gold nanomaterials have been used as drug delivery agents. The tumor targeting ligands associated with AuNPs have shown improved tumor targeting and enhanced cellular uptake efficiency. In addition to delivering

chemotherapeutic agents successfully to the tumor site, PEGylated AuNPs with human transferrin exert photothermal therapy upon irradiation. Taghdisi *et al.* [124] reported a modified polyvalent aptamers–Daunorubicin–AuNPs complex which exhibited efficient drug loading, tumor targeting, and controllable delivery of anticancer drug to tumor cells. Marques *et al.* [127] reported the polymeric AuNPs as a potential carrier system for drug delivery. Surface modification of AuNPs by polymers plays a significant role in conjugating the therapeutic entities for drug delivery via ionic, covalent bonding, or by physical adsorption. The anticancer drugs can be loaded in AuNPs by adopting various methods. For instance, the drug can be either attached to the capping agent or loaded inside the AuNPs. The AuNCs and AuNSs have higher drug loading efficiency due to the presence of hollow spaces. By utilizing these strategies, various therapeutic drugs have been successfully delivered using AuNCs and gold AuNSs. Many drugs including doxorubicin, paclitaxel, docetaxel, tamoxifen, oxaliplatin, and 3-mercaptopropionic acid have been successfully loaded in gold nanomaterials and used for anticancer therapy. Zhang *et al.* [128] reported the polymer encapsulated, doxorubicin-loaded AuNRs coupled the photothermal properties of AuNRs and the thermo and pH responsive properties of polymers. This nanocomposite provides an ideally versatile platform to simultaneously deliver heat and anticancer drugs in a laser-activation mechanism with facile control of the area, time, and dosage.

Iodice *et al.* [129] reported that poly (lactic acid-co-glycolic acid) (PLGA)-coated AuNPs exhibited direct cytotoxic effect on breast cancer cells (SUM-159) and in glioblastoma multiform cells (U87-MG). Betzer *et al.* [130] proposed a theranostic approach for the detection and therapy of head and neck cancer. Huang *et al.* [12] reported that plasmonic photothermal therapy acts as a promising cancer treatment and causes cell death, mainly via apoptosis and necrosis. The AuNRs displayed significant reduction in viability of breast, oral, and liver cancer cell lines. Yang *et al.* [131] reported that the chitosan-coated AuNRs tagged with siRNA (small interfering RNA) inhibited the oncogene expression in MDA-MB-231 triple-negative breast cancer cells, and moreover their anticancer efficacy was enhanced through NIR-mediated photothermal ablation. Zhong [132] reported FA-conjugated AuNRs were effectively used in photoacoustic therapy for selectively killing cancer cells within few seconds. Vo-Dinh *et al.* [78] reported photothermal ablation in SKBR3 cells by AuNSTs. Zou *et al.* [75] synthesized dual-aptamer-modified AuNSTs for photothermal therapy in prostate cancers. These studies have confirmed that

different types of gold nanomaterials act as promising materials for photothermal cancer application.



5. CONCLUSION AND PERSPECTIVES

On the whole, different types of gold nanomaterials including nanoparticles, nanorods, nanocages, nanostars, and nanoshells have shown multifunctional potential in tumor imaging, tumor targeting, and drug delivery and therapy. The synthesis of gold nanomaterials with tunable sizes and surface properties aims to reduce their toxicity, decrease their non-specific cellular uptake, and to increase their targeting efficiency. They are also used to improve the contrast in MRI and to enhance their load to target tumor cells in drug delivery. Their unique optical properties and their multifunctional potential to simultaneously diagnose and treat tumors enhance their reliability and versatility in the field of theranostics. The identification and synthesis of biocompatible cross-linking polymers will increase the stability and scope of gold nanomaterials in cancer treatment. The use of NIR rays and gold nanomaterials will be beneficial to target tumors that are located deep inside the body. To increase their half-life, stealth nanoparticles with improved characteristics have to be designed which will have prolonged circulation rates to facilitate the uptake of gold nanomaterials into cancer cells. The direction of future research regarding gold nanomaterials should focus on the need to overcome these hurdles and to develop novel therapies to provide solutions for the current problems. Promising clinical trials have given considerable hope that gold nanomaterials with improved characters help to develop safe and efficient tumor treatment/eradication methods in the near future.

REFERENCES

- [1] J. Ye, P. Van Dorpe, W. Van Roy, G. Borghs, G. Maes, Fabrication, characterization, and optical properties of gold nanobowl submonolayer structures, *Langmuir* 25 (2009) 1822–1827.
- [2] C.J. Murphy, L.B. Thompson, D.J. Chernak, J.A. Yang, S.T. Sivapalan, S.P. Boulos, J.Y. Huang, A.M. Alkilany, P.N. Sisco, Gold nanorod crystal growth: from seed-mediated synthesis to nanoscale sculpting, *Curr. Opin. Colloid Interface Sci.* 16 (2011) 128–134.
- [3] C.C. Li, K.L. Shuford, M.H. Chen, E.J. Lee, S.O. Cho, A facile polyol route to uniform gold octahedra with tailorable size and their optical properties, *ACS Nano* 2 (2008) 1760–1769.
- [4] M.Z. Liu, P. Guyot-Sionnest, Mechanism of silver(I)-assisted growth of gold nanorods and bipyramids, *J. Phys. Chem. B* 109 (2005) 22192–22200.

- [5] N.G. Khlebtsov, L.A. Dykman, Optical properties and biomedical applications of plasmonic nanoparticles, *J. Quant. Spectrosc. Radiat. Transf.* 111 (2010) 1–35.
- [6] C.L. Nehl, H.W. Liao, J.H. Hafner, Optical properties of star-shaped gold nanoparticles, *Nano Lett.* 6 (2006) 683–688.
- [7] C. Kim, E.C. Cho, J.Y. Chen, K.H. Song, L. Au, C. Favazza, Q.A. Zhang, C.M. Cobley, F. Gao, Y.N. Xia, L.H.V. Wang, In vivo molecular photoacoustic tomography of melanomas targeted by bioconjugated gold nanocages, *ACS Nano* 4 (2010) 4559–4564.
- [8] S.S. Shankar, A. Rai, A. Ahmad, M. Sastry, Rapid synthesis of Au, Ag, and bimetallic Au core-Ag shell nanoparticles using neem (*Azadirachta indica*) leaf broth, *J. Colloid Interface Sci.* 275 (2004) 496–502.
- [9] P. Mukherjee, A. Ahmad, D. Mandal, S. Senapati, S.R. Sainkar, M.I. Khan, R. Ramani, R. Parischa, P.A.V. Kumar, M. Alam, M. Sastry, R. Kumar, Bioreduction of AuCl₄⁽⁻⁾ ions by the fungus, *Verticillium sp.* and surface trapping of the gold nanoparticles formed D.M. and S.S. thank the Council of Scientific and Industrial Research (CSIR), Government of India, for financial assistance, *Angew. Chem. Int. Ed. Engl.* 40 (2001) 3585–3588.
- [10] M.C. Daniel, D. Astruc, Gold nanoparticles: assembly, supramolecular chemistry, quantum-size-related properties, and applications toward biology, catalysis, and nanotechnology, *Chem. Rev.* 104 (2004) 293.
- [11] S.S. Dash, B.G. Bag, Synthesis of gold nanoparticles using renewable *Punica granatum* juice and study of its catalytic activity, *Appl. Nanosci.* 4 (2012) 455–459.
- [12] P. Huang, L. Bao, C.L. Zhang, J. Lin, T. Luo, D.P. Yang, M. He, Z.M. Li, G. Gao, B. Gao, S. Fu, D.X. Cui, Folic acid-conjugated silica-modified gold nanorods for X-ray/Ct imaging-guided dual-mode radiation and photo-thermal therapy, *Biomaterials* 32 (2011) 9796–9809.
- [13] V.S. Marangoni, I.M. Paino, V. Zucolotto, Synthesis and characterization of jacalin-gold nanoparticles conjugates as specific markers for cancer cells, *Colloids Surf. B* 112 (2013) 380–386.
- [14] J.F. Hainfeld, F.A. Dilmanian, D.N. Slatkin, H.M. Smilowitz, Radiotherapy enhancement with gold nanoparticles, *J. Pharm. Pharmacol.* 60 (2008) 977–985.
- [15] M. Kodihla, E. Hutter, S. Boridy, M. Juhas, D. Maysinger, U. Stochaj, Gold nanoparticles induce nuclear damage in breast cancer cells: which is further amplified by hyperthermia, *Cell. Mol. Life Sci.* 71 (2014) 4259–4273.
- [16] J.W. Nichols, Y.H. Bae, EPR: evidence and fallacy, *J. Control. Release* 190 (2014) 451–464.
- [17] C.H.J. Choi, C.A. Alabi, P. Webster, M.E. Davis, Mechanism of active targeting in solid tumors with transferrin-containing gold nanoparticles, *Proc. Natl. Acad. Sci. U.S.A.* 107 (2010) 1235–1240.
- [18] S.E. Skrabalak, L. Au, X. Li, Y. Xia, Facile synthesis of Ag nanocubes and Au nanocages, *Nat. Protoc.* 2 (2007) 2182–2190.
- [19] X. Lu, J. Chen, S.E. Skrabalak, Y. Xia, Galvanic replacement reaction: a route to highly ordered bimetallic nanotubes, *J. Nanoeng. Nanosyst.* 221 (2008) 1–16.
- [20] S.E. Skrabalak, J. Chen, Y. Sun, X. Lu, L. Au, M. Cobley, Y. Xia, Gold nanocages: synthesis, properties, and applications, *Acc. Chem. Res.* 4 (2008) 1587–1595.
- [21] M.J. Kwon, J. Lee, A.W. Wark, H.J. Lee, Nanoparticle-enhanced surface plasmon resonance detection of proteins at attomolar concentrations: comparing different nanoparticle shapes and sizes, *Anal. Chem.* 84 (2012) 1702–1707.
- [22] M.A. Mahmoud, B. Snyder, M.A. El-Sayed, Surface Plasmon fields and coupling in the hollow gold nanoparticles and surface-enhanced Raman spectroscopy. Theory and experiment, *J. Phys. Chem. C* 113 (2010) 19475–19481.

- [23] L. Au, Y. Chen, F. Zhou, P.H.C. Camargo, B. Lim, Z.D.S. Ginger, Y. Xia, Synthesis and optical properties of cubic gold nanoframes, *Nano Res.* 4 (2008) 441–449.
- [24] M.A. Mahmoud, M.A. El-Sayed, Gold nanoframes: very high surface Plasmon fields and excellent near-infrared sensors *J. Am. Chem. Soc.* 132 (2010) 12704–12710.
- [25] E.C. Dreaden, A.M. Alkilany, X. Huang, C.J. Murphy, M.A. El-Sayed, The golden age: gold nanoparticles for biomedicine, *Chem. Soc. Rev.* 41 (2012) 2740–2779.
- [26] Y. Chen, Y. Zhang, W. Liang, X. Li, Gold nanocages as contrast agents for two-photon luminescence endomicroscopy imaging, *Nanomedicine* 8 (2012) 1267–1270.
- [27] R.D. Averitt, D. Sarkar, N.J. Halas, Plasmon resonance shifts of Au-coated Au₂S nanoshells: insight into multicomponent nanoparticle growth, *Phys. Rev. Lett.* 78 (1997) 4217–4220.
- [28] S.J. Oldenburg, R.D. Averitt, S.L. Westcott, N.J. Halas, Nano engineering of optical resonances, *Chem. Phys. Lett.* 288 (1998) 243–247.
- [29] R.D. Averitt, S.L. Westcott, N.J. Halas, Linear optical properties of gold nanoshells, *J. Opt. Soc. Am. B* 16 (1999) 1824–1832.
- [30] S.J. Oldenburg, J.B. Jackson, S.L. Westcott, N.J. Halas, Infrared extinction properties of gold nanoshells, *Appl. Phys. Lett.* 75 (1999) 2897–2899.
- [31] P. Tuersun, X. Han, Optical absorption analysis and optimization of gold nanoshells, *Appl. Opt.* 52 (2013) 1325–1329.
- [32] C. Loo, L. Hirsch, M. Lee, E. Chang, J. West, N. Halas, R. Drezek, Gold nanoshell bio-conjugates for molecular imaging in living cells, *Opt. Lett.* 30 (2005) 1012–1014.
- [33] J. Park, A. Estrada, K. Sharp, K. Sang, J.A. Schwartz, D.K. Smith, C. Coleman, J.D. Payne, B.A. Korgel, A.K. Dunn, J.W. Tunnell, Two-photon-induced photoluminescence imaging of tumors using near-infrared excited gold nanoshells, *Opt. Express* 16 (2008) 1590–1599.
- [34] L.R. Bickford, G. Agollah, R. Drezek, T. Yu, Silica-gold nanoshells as potential intra operative molecular probes for HER2-overexpression in ex vivo breast tissue using near-infrared reflectance confocal microscopy, *Breast Cancer Res. Treat.* 120 (2010) 547–555.
- [35] A.M. Gobin, M.H. Lee, N.J. Halas, W.D. James, R.A. Drezek, J.L. West, Near-infrared resonant nanoshells for combined optical imaging and photothermal cancer therapy, *Nano Lett.* 7 (2007) 1929–1934.
- [36] L.R. Hirsch, R.J. Stafford, J.A. Bankson, S.R. Sershen, B. Rivera, R.E. Price, J.D. Hazle, N.J. Halas, J.L. West, Nanoshell-mediated near-infrared thermal therapy of tumors under magnetic resonance guidance, *Proc. Natl. Acad. Sci. U.S.A.* 100 (2003) 13549–13554.
- [37] A.R. Lowery, A.M. Gobin, E.S. Day, N.J. Halas, J.L. West, Immuno nanoshells for targeted photothermal ablation of tumor cells, *Int. J. Nanomed.* 1 (2006) 149–154.
- [38] A.M. Gobin, J.J. Moon, J.L. West, Ephrinal-targeted nanoshells for photo thermal ablation of prostate cancer cells, *Int. J. Nanomed.* 3 (2008) 351–358.
- [39] H. Feng, C.L. Nehl, J.H. Hafner, P. Nordlander, Plasmon resonances of gold nanostars, *Nano Lett.* 7 (2007) 729–732.
- [40] L. Rodriguez-Lorenzo, R.A. Alvarez-Puebla, I. Pastoriza-Santos, S. Mazzucco, O. Stephan, M. Kociak, L.M. Liz-Marzan, F.J. Garcia de Abajo, Zeptomol detection through controlled ultrasensitive surface-enhanced Raman scattering, *J. Am. Chem. Soc.* 131 (2009) 4616–4618.
- [41] C. Hrelescu, T.K. Sau, A.L. Rogach, F. Jackela, F. Feldmann, Single gold nanostars enhance Raman scattering, *Appl. Phys. Lett.* 94 (2009) 153–183.
- [42] S.K. Dondapati, T.K. Sau, C. Hrelescu, T.A. Klar, F.D. Stefani, J. Feldmann, Label-free biosensing based on single gold nanostars as plasmonic transducers, *ACS Nano* 4 (2010) 6318–6322.

- [43] P. Mulvaney, Surface plasmon spectroscopy of nanosized metal particles, *Langmuir* 12 (1996) 788–800.
- [44] F. Schulz, T. Homolka, N.G. Bastus, V. Puntès, H. Weller, T. Vossmeier, Little adjustments significantly improve the turkevich synthesis of gold nanoparticles, *Langmuir* 30 (2014) 10779–10784.
- [45] M. Brust, J. Fink, D. Bethell, D.J. Schiffrin, C. Kiely, Synthesis and reactions of functionalized gold nanoparticles, *Chem. Commun.* 16 (1995) 1655–1656.
- [46] J.W. Park, J.S. Shumaker-Parry, Structural study of citrate layers on gold nanoparticles: role of intermolecular interactions in stabilizing nanoparticles, *J. Am. Chem. Soc.* 136 (2014) 1907–1921.
- [47] F. Westerlund, T. Bjornholm, Directed assembly of gold nanoparticles, *Curr. Opin. Colloid Interface Sci.* 14 (2009) 126–134.
- [48] R. Sardar, A.M. Funston, P. Mulvaney, R.W. Murray, Gold nanoparticles: past, present, and future, *Langmuir* 25 (2009) 13840–13851.
- [49] E. Boisselier, D. Astruc, Gold nanoparticles in nanomedicine: preparations, imaging, diagnostics, therapies and toxicity, *Chem. Soc. Rev.* 38 (2009) 1759–1764.
- [50] R.A. Sperling, P. Rivera Gil, F. Zhang, M. Zanella, W.J. Parak, Biological applications of gold nanoparticles, *Chem. Soc. Rev.* 37 (2008) 1896–1922.
- [51] J. Turkevich, P.C. Stevenson, J. Hillier, The formation of colloidal gold, *J. Phys. Chem.* 57 (1953) 670–673.
- [52] J. Turkevich, P.C. Stevenson, J. Hillier, A study of the nucleation and growth processes in the synthesis of colloidal gold, *Discuss. Faraday Soc.* 11 (1951) 55–75.
- [53] Y.Y. Yu, S.S. Chang, C.L. Lee, C.R.C. Wang, Gold nanorods: electrochemical synthesis and optical properties, *J. Phys. Chem. B* 101 (1997) 6661–6664.
- [54] N.R. Jana, L. Gearheart, C.J. Murphy, Wet chemical synthesis of high aspect ratio gold nanorods, *J. Phys. Chem. B* 105 (2001) 4065–4067.
- [55] K.R. Brown, D.G. Walter, M.J. Natan, Seeding of colloidal Au nanoparticle solutions. 2. Improved control of particle size and shape, *Chem. Mater.* 12 (2000) 306–313.
- [56] P.L. Gai, M.A. Harmer, Surface atomic defect structures and growth of gold nanorods, *Nano Lett.* 2 (2002) 771–774.
- [57] C.J. Johnson, E. Dujardin, S.A. Davis, C.J. Murphy, S. Mann, Growth and form of gold prepared by seed-mediated-directed synthesis, *J. Mater. Chem.* 12 (2002) 1765–1770.
- [58] J.X. Gao, C.M. Bender, C.J. Murphy, Dependence of the gold nanorod aspect ratio on the nature of the directing surfactant in aqueous solution, *Langmuir* 19 (2003) 9065–9070.
- [59] B. Nikoobakht, M.A. El-Sayed, Preparation and growth mechanism of gold nanorods (NRs) using seed-mediated growth method, *Chem. Mater.* 15 (2003) 1957–1962.
- [60] B.M.I. van der Zande, M.R. Bohmer, L.G.J. Fokkink, C. Schonenberger, Colloidal dispersions of gold rods: synthesis and optical properties, *Langmuir* 16 (2000) 451–458.
- [61] L.Y. Cao, T. Zhu, Z.F. Liu, Formation mechanism of nonspherical gold nanoparticles during seeding growth: Roles of anion adsorption and reduction rate, *J. Colloid Interface Sci.* 293 (2006) 69–76.
- [62] A. Gole, C.J. Murphy, Seed-mediated synthesis of gold nanorods: role of the size and nature of the seed, *Chem. Mater.* 16 (2004) 3633–3640.
- [63] N.R. Jana, L. Gearheart, C.J. Murphy, Seed-mediated growth approach for shape-controlled synthesis of spheroidal and Rod-like gold nanoparticles using a surfactant template, *Adv. Mater.* 13 (2001) 1389–1393.
- [64] L.F. Gou, C.J. Murphy, Fine-tuning the shape of gold nanorods, *Chem. Mater.* 17 (2005) 3668–3672.

- [65] N.D. Burrows, S. Harvey, F.A. Idesis, C.J. Murphy, Understanding the seed-mediated growth of gold nanorods through a fractional factorial design of experiments, *Langmuir* 33 (2017) 1891–1907.
- [66] C.J. Murphy, N.R. Jana, Controlling the aspect ratio of inorganic nanorods and nanowires, *Adv. Mater.* 14 (2002) 80–82.
- [67] S. Ross, C.E. Kwartler, J.H. Bailey, Colloidal association and biological activity of some related quaternary ammonium salts, *J. Colloid Sci.* 8 (1953) 385–401.
- [68] M.S. Bakshi, I. Kaur, Unlike surfactant–polymer interactions of sodium dodecyl sulfate and sodium dodecylbenzene sulfonate with water-soluble polymers, *Colloid Polym. Sci.* 281 (2003) 10–18.
- [69] S.B. Velegol, B.D. Fleming, S. Biggs, E.J. Wanless, R.D. Tilton, Counterion effects on hexa decyl trimethyl ammonium surfactant adsorption and self-assembly on silica, *Langmuir* 16 (2000) 2548–2556.
- [70] B. Nikoobakht, M.A. El-Sayed, Evidence for bilayer assembly of cationic surfactants on the surface of gold nanorods, *Langmuir* 17 (2001) 6368–6374.
- [71] Z. Wang, Z. Chen, Z. Liu, P. Shi, K. Dong, A multi-stimuli responsive gold nanocage hyaluronic platform for targeted photothermal and chemotherapy, *Biomaterials* 35 (2014) 9678–9688.
- [72] Y. Guan, X. Zheng, L. Jinglun, H. Zhenzhen, W. Yang, One-pot synthesis of size-tunable hollow gold nanoshells via APTES-in-water suspension, *Colloids Surf. A* 502 (2016) 6–12.
- [73] C.H. Kuo, M.H. Huang, Synthesis of branched of gold nanocrystals by a seeding growth approach, *Langmuir* 21 (2005) 2012–2016.
- [74] C.J. Murphy, N.R. Jana, Controlling the aspect ratio of inorganic nanorods and nanowires, *Adv. Mater.* 14 (2002) 80–82.
- [75] H. Zou, E. Ying, S. Dong, Seed-mediated synthesis of branched gold nanoparticles with the assistance of citrate and their surface-enhanced Raman scattering properties, *Nanotechnology* 17 (2006) 4758–4764.
- [76] H. Yuan, C.G. Khoury, Gold nanostars: surfactant-free synthesis, 3D modelling and two-photon photoluminescence imaging, *Nanotechnology* 23 (2012) 75–102.
- [77] L. Minati, One-step synthesis of star-shaped gold nanoparticles, *Colloids Surf. A* 441 (2014) 623–628.
- [78] C.G. Khoury, T. Vo-Dinh, Gold nanostars for surface-enhanced Raman scattering: synthesis, characterization and optimization, *J. Phys. Chem. C* 112 (2008) 18849–18859.
- [79] S. Barbosa, A. Agarwal, L.R. Lorenzo, L.M. Liz-Marzan, Size tuning and sensing capabilities of gold nanostars, *Langmuir* 26 (2010) 14943–14950.
- [80] J. Yu, D. Xub, G. Hua, W. Chao, H. Li, Facile one-step green synthesis of gold nanoparticles using *Citrus maxima* aqueous extracts and its catalytic activity, *Mater. Lett.* 166 (2016) 110–112.
- [81] G. Ghodake, S.R. Lim, D.S. Lee, Casein hydrolytic peptides mediated green synthesis of antibacterial silver nanoparticles. *Colloids Surf. B Biointerfaces* 108 (2013) 147–151.
- [82] W. Yana, C. Chena, L. Wanga, D. Zhang, Facile and green synthesis of cellulose nanocrystal-supported gold nanoparticles with superior catalytic activity, *Carbohydr. Polym.* 140 (2016) 66–73.
- [83] A. Nazirova, A. Pestova, Y. Privara, A. Ustinova, E. Modina, S. Bratskayaa, One-pot green synthesis of luminescent gold nanoparticles using imidazole derivative of chitosan, *Carbohydr. Polym.* 151 (2016) 649–655.
- [84] S. Suarasana, M. Focsana, O. Soritaub, D. Maniua, S. Astileana, One-pot, green synthesis of gold nanoparticles by gelatin and investigation of their biological effects on Osteoblast cells, *Colloids Surf. B Biointerfaces* 132 (2015) 122–131.

- [85] B. Sadeghi, M. Mohammadzadeh, B. Babakhani, Green synthesis of gold nanoparticles using *Stevia rebaudiana* leaf extracts: characterization and their stability, *J. Photochem. Photobiol. B* 148 (2015) 101–106.
- [86] C.G. Yuan, H. Can, Y. Shuixin, Biosynthesis of gold nanoparticles using *Capsicum annuum* var. *grossum* pulp extract and its catalytic activity, *Physica E* 85 (2017) 19–26.
- [87] D. Inbakandan, R. Venkatesan, S.A. Khan, Biosynthesis of gold nanoparticles utilizing marine sponge *Acanthella elongata*, *Colloids Surf. B Biointerfaces* 81 (2010) 634–639.
- [88] L. Castro, M.L. Blazquez, F. González, J.A. Munoz, A. Ballester, Extracellular biosynthesis of gold nanoparticles using sugarbeet pulp, *Chem. Eng. J.* 164 (2010) 92–97.
- [89] A.D. Dwivedi, K. Gopal, Biosynthesis of silver and gold nanoparticles using *Chenopodium album* leaf extract, *Colloids Surf. A* 369 (2010) 27–33.
- [90] K.P. Kumar, W. Paul, C.P. Sharma, Green synthesis of gold nanoparticles with *Zingiber officinale* extract: characterization and blood compatibility, *Process Biochem.* 46 (2011) 2007–2013.
- [91] M.M.H. Khalil, E.H. Ismail, F. El-Magdoub, Biosynthesis of Au nanoparticles using Olive leaf extract: 1st nano updates, *Arabian J. Chem.* 5 (2012) 431–437.
- [92] S. Kaviya, J. Santhanalakshmi, B. Viswanathan, Biosynthesis of silver nano-flakes by *Crossandra infundibuliformis* leaf extract, *Mater. Lett.* 67 (2012) 64–66.
- [93] V.G. Kumar, S.D. Gokavarapu, A. Rajeswari, T.S. Dhas, V. Karthick, Z. Kapadia, Facile green synthesis of gold nanoparticles using leaf extract of antidiabetic potent *Cassia auriculata*, *Colloids Surf. B Biointerfaces* 87 (2011) 159–163.
- [94] F. Cai, J. Li, J. Sun, Y. Ji, Biosynthesis of gold nanoparticles by biosorption using *Magnetospirillum gryphiswaldense* MSR-1, *Chem. Eng. J.* 175 (2011) 70–75.
- [95] K.M. Kumar, B.K. Mandal, M. Sinha, V. Krishnakumar, *Terminalia chebula* mediated green and rapid synthesis of gold nanoparticles, *Spectrochim. Acta A Mol. Biomol. Spectrosc.* 86 (2012) 490–494.
- [96] M. Noruzi, D. Zare, K. Khoshnevisan, D. Davoodi, Rapid green synthesis of gold nanoparticles using *Rosa hybrida* petal extract at room temperature, *Spectrochim. Acta A Mol. Biomol. Spectrosc.* 79 (2011) 1461–1465.
- [97] T.Y. Suman, S.R.R. Rajasree, R. Ramkumar, C. Rajthilak, P. Perumal, The green synthesis of gold nanoparticles using an aqueous root extract of *Morinda citrifolia* L., *Spectrochim. Acta A Mol. Biomol. Spectrosc.* 118 (2014) 11–16.
- [98] B. Ankamwar, M. Chaudhary, M. Sastry, Gold nanotriangles biologically synthesized using tamarind leaf extract and potential application in vapor sensing, *Nano-Met. Chem.* 35 (2005) 19–26.
- [99] P.P. Gan, S.H. Ng, Y. Huang, S. Fong, Y. Li, Green synthesis of gold nanoparticles using palm oil mill effluent (POME): a low-cost and eco-friendly viable approach, *Bio-resour. Technol.* 113 (2012) 132–135.
- [100] T. Klaus, R. Joerger, E. Olsson, C.G. Granqvist, Silver-based crystalline nanoparticles, microbially fabricated, *Proc. Natl. Acad. Sci. U.S.A.* 96 (1999) 13611.
- [101] T.J. Beveridge, R.G.E. Murray, Sites of metal deposition in the cell wall of *Bacillus subtilis*, *J. Bacteriol.* 141 (1980) 876.
- [102] Y. Konishi, T. Tsukiyama, Room-temperature synthesis of gold nanoparticles and nanoplates using *Shewanella algae* cell extract, *Electrochim. Acta* 53 (2007) 186.
- [103] N. Pugazhenthiran, S. Anandan, G. Kathiravan, N.K.U. Prakash, Microbial synthesis of silver nanoparticles by *Bacillus* sp., *J. Nanopart. Res.* 11 (2009) 1811.
- [104] V. Yadav, N. Sharm, Generation of selenium containing nano-structures by soil bacterium, *Pseudomonas aeruginosa*, *Biotechnology* 7 (2008) 299.
- [105] L. Wen, Z. Lin, P. Gu, Extracellular biosynthesis of monodispersed gold nanoparticles by a SAM capping route, *J. Nanopart. Res.* 11 (2009) 279.

- [106] B. Zhoua, Y. Jia, PEGylated polyethylenimine-entrapped gold nanoparticles modified with folic acid for targeted tumor CT imaging, *Colloids Surf. B Biointerfaces* 140 (2016) 489–496.
- [107] C. Gui, D. xiang, Functionalized gold nanorods for tumor imaging and targeted therapy, *Cancer Biol. Med.* 9 (2012) 221–233.
- [108] H. Yuan, Gold nanostars: surfactant-free synthesis, 3D modelling, and two-photon photoluminescence imaging, *Nanotechnology* 23 (2012) 75102.
- [109] M. Lengke, M.E. Fleet, G. Southam, Morphology of gold nanoparticles synthesized by filamentous cyanobacteria from gold (I)-thiosulfate and gold (III)-chloride complexes, *Langmuir* 22 (2006) 2780.
- [110] M. Lengke, B. Ravel, M.E. Fleet, G. Wanger, Mechanisms of gold bioaccumulation by filamentous cyanobacteria from gold (III)-chloride complex, *Environ. Sci. Technol.* 40 (2006) 6304.
- [111] L. Du, H. Jiang, H. Xiaohua, E. Wang, Biosynthesis of gold nanoparticles assisted by *Escherichia coli* DH5 α and its application on direct electrochemistry of hemoglobin, *Electrochem. Commun.* 9 (2007) 1165.
- [112] Y. Feng, Y. Yu, Y. Wang, Biosorption and bioreduction of trivalent aurum by photosynthetic bacteria *Rhodobacter capsulatus*, *Curr. Microbiol.* 55 (2007) 402.
- [113] R. Joerger, T. Klaus, C.G. Granqvist, The biochemistry of apoptosis, *Adv. Mater.* 12 (2000) 407.
- [114] B. Zhou, Y. Jia, PEGylated polyethylenimine-entrapped gold nanoparticles modified with folic acid for targeted tumor CT imaging, *Colloids Surf. B Biointerfaces* 140 (2016) 489–496.
- [115] N. Lozano, T. Wafa, A. Jamal, Liposome-gold nanorod hybrids for high-resolution visualization deep in tissues, *J. Am. Chem. Soc.* 134 (2012) 13256–13258.
- [116] X. Huang, A reexamination of active and passive tumor targeting by using rod shaped gold nanocrystals and covalently conjugated peptide ligands, *ACS Nano* 4 (2010) 5887–5896.
- [117] M.E. Gallina, Y. Zhou, J. Christopher, Aptamer-conjugated, fluorescent gold nanorods as potential cancer theradiagnostic agents, *Mater. Sci. Eng. C* 59 (2016) 324–332.
- [118] H. Wang, In vitro and in vivo two-photon luminescence imaging of single gold nanorods, *Proc. Natl. Acad. Sci. U.S.A.* 102 (2005) 15752–15756.
- [119] W. Li, In vivo quantitative photoacoustic microscopy of gold nanostars kinetics in mouse organs, *Biomed. Opt. Express* 5 (2014) 2679–2685.
- [120] C.H. Lee, Near-infrared mesoporous silica nanoparticles for optical imaging: characterization and in vivo distribution, *Adv. Funct. Mater.* 19 (2009) 7688–7693.
- [121] S. Ye, Label-free imaging of zebrafish larvae in vivo by photoacoustic microscopy, *Biomed. Opt. Express* 3 (2012) 360–365.
- [122] L. Nie, Plasmonic nanostars: in vivo volumetric photoacoustic molecular angiography and therapeutic monitoring with targeted plasmonic nanostars, *Small* 10 (2014) 1585–1593.
- [123] S.M. Taghdisi, N.M. Danesh, Double targeting, controlled release and reversible delivery of daunorubicin to cancer cells by polyvalent aptamers-modified gold nanoparticles, *Mater. Sci. Eng. C* 61 (2016) 753–761.
- [124] Z. Yang, T. Liu, X. Yan, Chitosan layered gold nanorods as synergistic therapeutics for photothermal ablation and gene silencing in triple-negative breast cancer, *Acta Biomater.* 25 (2015) 194–204.
- [125] D.H. Dam, Direct observation of nanoparticles-cancer cell nucleus interaction, *ACS Nano* 6 (2012) 3318–3326.
- [126] D.H. Dam, Shining light on nuclear-targeted therapy using gold nanostars constructs, *Ther. Deliv.* 3 (2012) 1263–1267.

- [127] T. Marques, M. Schwarcke, Gel dosimetry analysis of gold nanoparticle application in kilovoltage radiation therapy, *J. Geophys. Res.* 250 (2010) 12084.
- [128] Z. Zhang, J. Wang, X. Nie, Near infrared laser-induced targeted cancer therapy using thermoresponsive polymer encapsulated gold nanorods, *J. Am. Chem. Soc.* 136 (2014) 7317–7326.
- [129] C. Iodice, Enhancing photothermal cancer therapy by clustering gold nanoparticles into spherical polymeric nanoconstructs, *Opt. Lasers Eng.* 76 (2016) 74–81.
- [130] O. Betzer, R. Ankri, M. Motiei, R. Popovtzer, Theranostic approach for cancer treatment: multifunctional gold nanorods for optical imaging and photothermal therapy, *J. Nanomater.* 5 (2015) 646713.
- [131] L. Yang, Quintuple-modality (SERS-MRI-CT-TPL-PTT) plasmonic nanoprobe for theranostics, *Nanoscale* 5 (2013) 12126.
- [132] J. Zhong, Imaging-guided high-efficient photoacoustic tumor therapy with targeting gold nanorods, *Nanomedicine* 11 (2015) 1499–1509.

INDEX

Note: Page numbers followed by “*f*” indicate figures, and “*t*” indicate tables.

A

Acid sphingomyelinase (ASM), 58
Acyl chain structures, 54
Amino acid encapsulation, 74–75
Amino acids arginine, 75*f*
Amphiphile–aqueous solution system
 inverse bicontinuous cubic phases, 64–66, 64*f*
Amphiphilic amino acids, 74–75
Amphiphilic enzyme, 87
Aneurysms, 4
Anisotropy, 133–134
Antimicrobial peptides (AMPs), 77–78, 112–113
 aurein 1.2, 150–151, 151*f*
 birefringence changes, 148–150, 149*f*
 cubosomes, 112–113
 DMPC, 149*f*, 150–151
 magainin 2 (Mag2), 150–151, 151*f*
 membrane destruction, 150–151
AP114 peptide, 78–79
Aspirin, 56–57
Atheromatous plaques, 4
Atherosclerosis (ASc), 4–5
Atherosclerotic renovascular disease (ARVD), 6
Atomic force microscopy (AFM), 99–100
AuNCgs. *See* Gold nanocages (AuNCgs)
AuNPs. *See* Gold nanoparticles (AuNPs)
AuNRs. *See* Gold nanorods (AuNRs)
AuNShs. *See* Gold nanoshells (AuNShs)
AuNSts. *See* Gold nanostars (AuNSts)

B

Bacteriorhodopsin (bR), 84–85, 84*f*
Bare-metal stents (BMS), 9–10
 β 2 adrenergic receptor, 84*f*
Bicontinuous cubic phases, 108–111
Bilayer thicknesses, 98–99
Bile acids, 57
Biocompatibility, 12–13
Biofilms, 33

Biomembranes, 126, 128
Biomolecule system *vs.* lipidic cubic phase, 66, 66*f*
Birefringence, 133–135
Bivariate K–function analysis, 50–52, 51*f*
bR. *See* Bacteriorhodopsin (bR)

C

Caillé theory, 98–99
Cardiovascular diseases (CVDs)
 atherosclerosis (ASc), 4–5
 risk factors, 3
 vascular implant, 2–3
Carotid artery disease, 5–6
Casein hydrolytic peptides (CHPs), 167–168
Caveolae, 55
Cetyltrimethyl ammonium bromide (CTAB), 165
Cholesterol, 99–100, 142
CHPs. *See* Casein hydrolytic peptides (CHPs)
Coronary heart disease (CHD), 5
Critical micelle concentrations (CMCs), 57, 109–111
Critical packing parameter (CPP)
 lipidic mesophases, 109–111
 values of lipids, 67–68, 67*f*
Cryogenic transmission electron microscopy (cryo-TEM), 74
CTAB. *See* Cetyltrimethyl ammonium bromide (CTAB)
Cubic phase nanoparticles, 71–73
Cubosomes, 71–73, 72*f*, 111–113
Curcumin, 112–113
Curvature-dependent selectivity, 115–116
Curved membranes
 curvature-dependent selectivity, 115–116
 lipidic mesophases
 bicontinuous cubic phases, 108–111
 critical packing parameter (CPP), 109–111
 mean curvature, 109–111

- Curved membranes (*Continued*)
 molecular shapes, 109–111
 monoglycerides, 108–109
 mesosomes
 applications, 112–113
 cubosomes, 111–113
 curcumin, 112–113
 hexosomes, 111
 pluronic F127, 111
 quercetin, 113–115, 114*f*
 small-angle X-ray scattering (SAXS),
 113–114, 114*f*
 structural analysis of, 112*f*
- D**
 DAPI staining, 29
 De Feijter formula, 135
 DES. *See* Drug-eluting stents (DES)
 Dioleoylphosphatidylcholine (DOPC), 102
 Dipalmitoylphosphatidylcholine
 (DPPC), 102
 Divalent cations, 143–144
 D2L dopamine receptor, 84–85
 DMPC, 143
 DPK-060 peptide, 78–79
 Drug-eluting stents (DES), 9–11, 23
 Dual polarization interferometry (DPI)
 anisotropy, 132–135
 birefringence, 132–135
 instrumentation, 129–131
 lipid molecular organization, changes in
 antimicrobial peptides (AMPs),
 148–152
 birefringence changes, 148–150, 149*f*
 multistructural parameters, 147–148
 operating principle, 129–131
 optogeometrical parameters, 135
 polarization modes, 131–132, 132*f*
 supported lipid bilayers (SLBs)
 biomembrane layer preparation,
 136–138
 challenges, 145–146
 divalent cations, 143–144
 ionic strength, 143
 limitations, 145–146
 liposomes, 138–141
 modified chip, anchored liposomes on,
 146–147
 osmotic pressure, 145
 pH, 144–145
 salt, 143–144
 substrate, 138
 temperature, 142
 Dynamic light scattering (DLS)
 spectroscopy, 74
- E**
 Electrochemical anodization, 12–13
 TiO₂ fabrication, 19
 Elyzol Dental Gel, 70–71
 Encapsulated proteins, 66
 Encapsulation. *See specific types of encapsulation*
 Endothelial cells (EC)
 culturing, 28
 human coronary artery endothelial cells
 (HCAEC), 27–28, 28*f*, 30*f*
 immunofluorescent microscopy, 28–29
 staining, 29
 vascular stent, 27
 Endovascular stent-grafting, 9
 Epidermal growth factor (EGF), 46–47
Escherichia coli, 168–170
 ClC transporter protein, 87
- F**
 Fabricated nanotubes (NTs), 16
 Fendiline, 57–58
 Flavonoid-lipid interactions
 with curved membranes
 curvature-dependent selectivity,
 115–116
 lipidic mesophases, in bulk, 108–111
 mesosomes, 111–115, 112*f*, 114*f*
 with planar membranes
 functions, 98–100
 influence, 100–108, 103–107*t*
 structures, 98–100
 Fluorescein phalloidin, 28–29
 Fluorescence recovery after photobleaching
 (FRAP), 73–74, 86
 Fluorescence resonance energy transfer
 (FRET), 43–45
 Food and Drug Administration (FDA),
 22–23
 FRAP. *See* Fluorescence recovery after
 photobleaching (FRAP)

G

- Gaseous plasma
 - in medical applications, 19–21
 - TiO₂ nanotubes, 21
 - treatment, 16–17
- G-domain conformational orientation, 49–50
- GDP-bound H-Ras, 49
- Geobacter ferrireducens*, 168–170
- GFP-LactC2 probe, 57–58
- Giant plasma membrane vesicles (GPMVs), 57
- Gold nanocages (AuNCgs), 163–164
 - synthesis of, 165–166
- Gold nanomaterials, 162–164
 - diagnostic and imaging applications of, 170–171
 - synthesis of
 - chemical-mediated, 164–167
 - green, 167–168, 168*t*
 - microbial, 168–170, 169*t*
 - therapeutic and drug delivery applications of, 171–173
- Gold nanoparticles (AuNPs), 162
 - PEGylated, 171–172
 - shape types, 163*f*
 - surface modification of, 171–172
 - synthesis of, 164–165
 - tracking of, 171
- Gold nanorods (AuNRs), 163
 - bioconjugation of, 170–171
 - synthesis of, 165
- Gold nanoshells (AuNSHs), 164
 - synthesis of, 166
- Gold nanostars (AuNSts), 164
 - synthesis of, 166–167
 - TPACS of, 171
- Gramicidin A, 76–77, 76*f*
- Green synthesis, of gold nanomaterials, 167–168, 168*t*

H

- Heptapeptides, 81
- Hexosomes, 111
- Hydrophilic moieties, 65–66

I

- Indomethacin, 56–57
- Infrared reflection absorption spectroscopy (IRRA), 50
- In meso crystallization, 69–70, 86
- Integral membrane protein encapsulation, 83–87
- Interfacial curvature, 67–68
- ISAsomes. *See* Mesosomes
- Ischemia, 5–6

L

- Lateral pressure, 67–68
- Lipid(s), 68*f*
 - anchors
 - atomic force microscopy (AFM), 48–49
 - H-Ras, 48
 - K-Ras, 48–49
 - methyl- β -cyclodextrin (M β CD), 48
 - N-Ras, 48–49
 - CPP values of, 67–68, 67*f*
 - inverse bicontinuous cubic phases in pure, 64*f*
 - wedge-shaped, 67–68
- Lipid A phosphoethanolamine transferase (LptA), 87
- Lipidic cubic phase *vs.* biomolecule system, 66, 66*f*
- Lipid mesophase, 74, 76
 - physicochemical parameters of, 67
 - structural parameters of, 70–71
- Lipid packing, 67–68
- Liposomes
 - birefringence, 140–141
 - mechanical extrusion, 138–140
 - on modified chip, 146–147
 - osmotic pressure, 145
 - POPC SLBs formation, 140–141, 141*f*
 - unilamellar, 138–139
 - vesicle-to-SLB transformation, 139
- LL-37 peptide, 78–79
- Localized surface plasmon resonance (LSPR), 162–166
 - of AuNRs, 165
- Lyotropic liquid crystalline systems, 96–97

M

- MAPK signal transduction, 46–47, 47*f*
 Maxwell's equations, 131–132
 M β CD. *See* Methyl- β -cyclodextrin (M β CD)
 Membrane fluidity, 102–108, 103–107*t*
 Membrane proteins, 65–66, 69–70, 80, 82, 84–87
 Mesenchymal stem cells (MSCs), 30–32, 31*f*
 Mesophase, 74, 77, 79–80, 87
 in excess water condition, 96–97
 phase behavior of, 85
 structural evolution of, 86
 Mesosomes
 applications, 112–113
 cubosomes, 111–113
 curcumin, 112–113
 hexosomes, 111
 pluronic F127, 111
 quercetin, 113–115, 114*f*
 small-angle X-ray scattering (SAXS), 113–114, 114*f*
 structural analysis of, 112*f*
 Methyl- β -cyclodextrin (M β CD), 48–49
 Monoacylglycerols, 65
 Monoglycerides, 108–109
 Monoolein, 79–80, 84–85
 Monopalmitolein system, 86
 Multilamellar vesicles (MLVs), 97–98
 Multistructural parameters, 147–148

N

- Nanotopography, 11–12
 Near-infrared (NIR) light, 162
 Nonbilayer-forming lipids, 115–116
 Nonsteroidal antiinflammatory drugs (NSAIDs), 56–57
 Nonthermal plasmas, 19–21

O

- Oleylethanolamide-based cubic phase system, 75
 Optical biosensor, 127–128, 131
 Orthogonal polarization, 131, 133–134
 transverse electric (TE) mode, 131–132, 132*f*

- transverse magnetic (TM) mode, 131–132, 132*f*

Osmotic pressure, 145

Osteoblasts, 13

P

- 1-Palmitoyl-sn-glycero-3-phosphocholine (PLPC) cubic phase, 78
 Peptide encapsulation, 66, 76–83
 applications of bicontinuous cubic phases for
 drug delivery, 70–71
 in meso crystallization, 69–70
 Peptides melittin, 76*f*
 Percutaneous transluminal angioplasty (PTA), 7–8
 Peripheral artery disease (PAD), 6
 Phase transition temperature, 142
 Phenylalanine, 74–75
 Phosphatidylethanolamine (PE), 52–53
 Phosphatidylserine (PS)
 acyl chain structures, 54–55
 of K-Ras nanoclusters, 52–54, 52*f*
 Phosphoethanolamide, 87
 Phosphoinositol 3-kinase (PI3K), 45–46
 Phospholipids, 97–100
 Phytantriol, 65
 Planar lipid bilayers, 97–98
 atomic force microscopy (AFM), 99–100
 bilayer thicknesses, 98–99
 cholesterol, 99–100
 dioleoylphosphatidylcholine (DOPC), 102
 dipalmitoylphosphatidylcholine (DPPC), 102
 flavonoids, 101–102
 in fluid phase (L α), 98–99
 fluorescence anisotropic measurements, 101
 in gel phase (L β), 99
 liquid-ordered phases, 99–100
 membrane fluidity, 102–108, 103–107*t*
 Plasma membrane (PM) depolarization, 53–54
 Plasma modification, 19–21
 Plasma reactor, 21, 22*f*
 Plasma sterilization, 19–21
 Platelets, 23–27, 24*f*

- incubation, with whole blood, 24–25
SEM analysis, 25–27, 26*f*
- Plectonema boryanum*, 168–170
- Pluronic F127, 111
- Polyethylenimine (PEI), 170
- Protein
- bicontinuous cubic phase,
 - characterization of, 73–87
 - membrane, 84–87
 - transmembrane domain of, 85
- Protein encapsulation, 66
- applications of bicontinuous cubic phases
 - for, 69
 - drug delivery, 70–71
 - in meso crystallization, 69–70
 - integral membrane, 83–87
- Protein ompF porin, 87
- PS synthases (PSS), 52–53
- Q**
- Quercetin, 113–115, 114*f*
- R**
- Ras nanoclusters
- acidic lipid selectivity, 50–55
 - alters Ras effector binding and signaling,
 - 56–58
 - on cell plasma membrane, 42–45
 - definition, 42–43
 - electron microscopy (EM), 43–45, 44*f*
 - fluorescence resonance energy transfer (FRET), 43–45, 45*f*
 - H-Ras, 42–43
 - isoforms, 42–43
 - K-Ras, 42–43
 - MAPK signal transduction, 45–47, 47*f*
 - N-Ras, 42–43
 - ordered *vs.* disordered domains, in
 - cell PM
 - G-domain conformational orientation, 49–50
 - lipid anchors, 48–49
 - signal mechanisms, 43–45
 - spatial distribution, 43–45
- Rhodobacter capsulatus*, 168–170
- S**
- SAXS. *See* Small angle X-ray scattering (SAXS) spectroscopy
- Scanning electron microscopy (SEM), 16, 16*f*
- Silicon oxynitride chip, 129, 138
- Small angle X-ray scattering (SAXS) spectroscopy, 73–74, 113–114, 114*f*
- Smooth muscle cells (SMCs), 9–11
- Sphingolipids, 142
- Stable plaques, 4
- Stent-grafts, 9
- Stevia rebaudiana*, 167–168
- Structural coloration, 96–97
- Supported lipid bilayers (SLBs)
- biomembrane layer preparation, 136–138
 - challenges, 145–146
 - divalent cations, 143–144
 - ionic strength, 143
 - limitations, 145–146
 - liposomes, 138–141
 - modified chip, anchored liposomes on,
 - 146–147
 - osmotic pressure, 145
 - pH, 144–145
 - salt, 143–144
 - substrate, 138
 - temperature, 142
- Surface modification, 12–13
- Surface wettability, 18, 18*f*
- Synthetic peptide WLFLKKK, 81
- T**
- Thermal plasmas, 19–21
- Thrombosis, 23
- Ti foil, 17–18
- Titanium dioxide (TiO₂) nanotubes
- antiinfective properties, 32–33
 - electrochemical anodization, 12–13
 - growth of, 15, 15*t*
 - interaction
 - endothelial cells (EC), 27–29, 28*f*, 30*f*
 - mesenchymal stem cells (MSCs),
 - 30–32, 31*f*
 - platelets, 23–27, 24*f*
 - surface modification
 - gaseous plasma, 19–21, 22*f*

- Titanium dioxide (TiO₂) nanotubes
(*Continued*)
 plasma-modified NTs, 22
 surface properties
 chemistry, 16–18, 17*f*
 morphology, 16, 16*f*
 wettability, 18, 18*f*
- Tryptophan, 74–75, 75*f*
- Two-photon action cross sections (TPACS)
 of nanostars, 171
- U**
- UV-ozone cleaning, 138
- V**
- Vascular grafts
 bypass grafting, 8–9
 polyethylene terephthalate, 8–9, 8*f*
 polytetrafluoroethylene, 8–9, 8*f*
- Vascular implants
 atherosclerosis (ASc), 4–5
 atherosclerotic renovascular disease (ARVD), 6
 biocompatibility, 12–13
 carotid artery disease, 5–6
 coronary heart disease (CHD), 5
 nanotopography, 11–12
 peripheral artery disease (PAD), 6
 surface modification, 12–13
 titanium dioxide (TiO₂) nanotubes
 antiinfective properties, 32–33
 growth of, 15, 15*t*
 interaction, 22–32, 24*f*, 26*f*, 28*f*, 31*f*
 surface modification, 19–22, 22*f*
 surface properties, 16–18, 16*f*, 18*f*
- types
 grafts, 8–9, 8*f*
 stent-graft, 9
 stents, 7–11, 7*f*
- Vascular stents
 angioplasty, 7–8
 complications, 9–11
 definition, 7
 metal structures, 7
- W**
- WALP peptides, 80
WALPS53 peptides, 80–81
WALPS73 peptides, 80–81
Wedge-shaped lipids, 67–68
- X**
- X-ray photoelectron spectroscopy (XPS),
 16–18, 17*f*

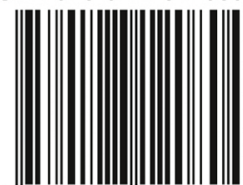
Cover image: Structural analysis of mesosomes formulated with 10 w% Dimodan U/J (an industrial source of monoglyceride) and stabilized by 0.5 w% F127 block copolymer. A) Size distribution curve obtained from light scattering experiments showing the formation of about 300 nm-sized droplets. B) A schematic representation of the droplet interface and a proposed molecular organisation demonstrating the co-existence of fluid lamellar and cubic phase. C) 3-D electron density map reconstructed from the small angle X-ray scattering data of empty cubosomes.



ACADEMIC PRESS

An imprint of Elsevier
elsevier.com/books-and-journals

ISBN 978-0-12-812080-4



9 780128 120804